Percolative metal-organic framework/carbon composites for hydrogen storage

CrossMark

Shuqian Xie [a], Jiann-Yang Hwang [b], Xiang Sun [b], Shangzhao Shi [b], Zheng Zhang [b], Zhiwei Peng [b], Yuchun Zhai [a,*]

[a] School of Materials and Metallurgy, Northeastern University, No. 11, Lane 3, Wenhua Road, Heping District, Shenyang, Liaoning 110819, China
[b] Department of Materials Science and Engineering, Michigan Technological University, 1400 Townsend Drive, Houghton, MI 49931, USA

HIGHLIGHTS

- We study hydrogen adsorption over MOFs by introducing an external electric field.
- We synthesize activated carbon additive and MOF composites.
- The hydrogen uptake capability is increased with help from the PMN-PT.
- Electrostatic interaction between hydrogen and adsorbent can be built by external electric field.

ARTICLE INFO

ABSTRACT

Percolative Metal-organic framework/Carbon (MOFAC) composites are synthesized by IRMOF8 (iso-reticular metal-organic frameworks) directly depositing on activated carbon via heterogeneous nucleation. Carbon content is calculated by TGA (Thermogravimetric analysis) tests. XRD (X-ray diffraction) and FESEM (Field emission-scanning electron microscope) are carried out to characterize the structures of the samples. BET surface areas and the pore size distribution are measured. The dielectric constant is measured with impedance analyzer and a specially designed sample holder. The dielectric constants of the MOFAC composites rise with increasing the carbon content, and the composites possess the insulator−conductor transition as the carbon content increases from 17.77 wt% to 22.2 wt%. The composites are further tested for hydrogen storage capability under assist of the PMN-PT (single crystal lead magnesium niobate−lead titanate) generated electric field. With help from the PMN-PT, the hydrogen uptake capability is increased about 31.5% over the MOFAC3 (MOF-Carbon composite with 22.2 wt% of carbon) without PMN-PT, which is elucidated by the charge distribution mechanisms. The improved storage is due to a stronger electrostatic interaction between IRMOF8 and hydrogen molecule caused by field polarization. Meanwhile, rapid adsorption/desorption kinetics and total reversibility on the samples are observed in the present or absence of external electric field.

© 2013 Elsevier B.V. All rights reserved.

1. Introduction

The largest obstacle for utilizing hydrogen energy for transportation applications is the reversible storage of hydrogen gas in vehicles. With respect to the gas physisorption, various adsorbents such as activated carbon [1–3], carbon nanostructures [4–6], and zeolites [7] have been extensively studied over the past few decades. However, at ambient temperature, none of these adsorbents can be used for transportation applications. Recently, a new class of porous materials, namely metal-organic frameworks (MOFs) has been developed which have an extremely large surface area and potential applications as adsorbents [8]. The weak adsorption energy limits MOF's real hydrogen storage applications although promising storage capacity has been achieved at 77 K [9–11]. Hydrogen spillover has remarkably increased the storage capacity of IRMOF8 to 4 wt% at room temperature [12,13], however, the strong interaction energy results in problems such as slow adsorption/desorption kinetics, and questionable reversibility.

Our group has reported a novel way to increase hydrogen adsorption enthalpy in carbon [14,15] and oxide materials [16] by using an external electric field. Promising enhancement has been achieved and our computational work [17] also supports these observations. Moreover, a publication [18] from another group also demonstrated the storage enhancement effect of an electric field in

graphenes. To date, such approach has not been employed with MOF materials. Since most MOF materials are not electrically conductive, the charges cannot be distributed throughout every particle. Therefore, adding conductive agents into MOFs without significantly affecting the total porosity is critical to realizing charge enhancement in MOF materials.

Percolation is a method of adding conductive materials (filler) into a non-conductive polymer or ceramics (matrix) to alter the dielectric properties [19,20] of the matrix. The percolative composites composed of carbon materials/PVDF [21], CNT/ceramics [22,23], and CNT/BaTiO$_3$ [24] all showed promising improvement of their dielectric constants.

In this study, IRMOF8 was directly deposited onto activated carbon to form a percolative MOF-activated carbon composite, following the theory of heterogeneous nucleation. The dielectric constant of the composites was evaluated and, as the carbon content increased, a significant enhancement was observed. Moreover, the composites were tested for hydrogen storage with and without the presence of the charge generating material PMN-PT (single crystal lead magnesium niobate–lead titanate). The significant enhancement was achieved when the composite followed the insulator to conductor transition.

2. Experimental

2.1. Preparation of MOF-carbon composites

IRMOF8 was synthesized on activated carbon by using the DMF approach [13,25,26]. Zn(NO$_3$)$_2$·6H$_2$O (1.19 g) was dissolved in 40 ml DMF (N,N′-dimethylformamide) with magnetic stirring. Various amount of powdered Norit A Supra (Norit Corporation) activated carbon (0.2 g, 0.35 g and 0.4 g) were added to the solution. 2,6-Napthalene dicarboxylic acid (0.43 g) was then added and stirred until dissolved. Three drops of hydrogen peroxide (30 wt%) solution was added. Then Triethylamine (2.3 ml) was added dropwise and the solution was stirred for 1 h. The IRMOF8 product was recovered by repetitive filtration and DMF washing for three times. It was then degassed at room temperature for 6 h and heated to 180 °C at a heating rate of 1 °C min^{-1}, and kept overnight in a box vacuum furnace (Precision).

Depending on the amount of activated carbon used for synthesis, the samples were denoted as MOFAC1, MOFAC2, and MOFAC3, respectively.

2.2. Characterization

Thermogravimetric analysis (TGA) was performed under nitrogen flow at a heating rate of 10 °C min^{-1} from 25 °C to 600 °C by using an SDT Q600 V8.3 Build 101 (TA Instruments). X-ray diffraction (XRD) measurement was carried out with a Scintag XDS2000 Powder Diffractometer at a scan rate of 0.08° s^{-1} with Cu radiation at 45 kV, 35 mA. A Hitachi S-4700 field emission-scanning electron microscope (FE-SEM) was used to examine the microstructure of the samples. The surface area and pore size distribution were measured using a Micromeritics ASAP2000 instrument. The samples were evacuated by heating at 200 °C under vacuum for 12 h before testing.

The dielectric constant was measured using an HP 4192A LF impedance analyzer with a specially designed sample holder [27]. As shown in Fig. 1, the sample holder consists of two metal parts, each connected to the analyzer through electrical wires. The PVDF ring was placed into the bottom steel holder, leaving the center circle (one inch in diameter and 0.0625 inch in depth) open. The samples were loosely packed in the PVDF ring and covered by the top steel holder for the measurement. This kind of arrangement is
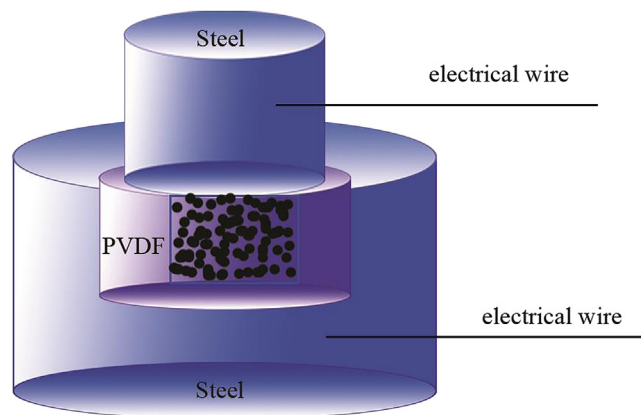

Fig. 1. Schematic of the holder used for dielectric constant measurements.

essential to a comparable analysis with the hydrogen storage measurement, where the sample powders were loosely placed inside the storage sample holder. The electrical resistivity was measured with a digital multimeter (Agilent 34405 A).

2.3. Hydrogen storage measurement

Hydrogen adsorption at pressures between 0.1 bar and 140 bar was measured by using static volumetric techniques with an automatic Sieverts' apparatus (PCT-Pro 2000 from Hy-Energy LLC) at room temperature. Prior to the test, samples were degassed extensively at 200 °C for 12 h and then carefully moved into the sample holder and evacuated again at 100 °C for 2 h to ensure removal of any contamination on the sample surface. Approximately 100–300 mg sample was used in each test, and ultra pure (99.999%) hydrogen and helium gases were used for all calibrations and measurements.

Single crystal PMN-PT disks were acquired from Morgan Electro Ceramics, 5 mm in length and width, and 1 mm in thickness. For the conductive samples, the positive side of the PMN-PT was covered by a non-conductive thin BaTiO$_3$ film made by BaTiO$_3$ powders and glue to prevent electron transfer from the negative side to the positive side. The coated PMN-PT was then immersed in the adsorbents for measurements. For the non-conductive samples, the plain PMN-PT was directly immersed in the samples. A glass container was used to ensure good electric insulation from the outside steel holder. In such an arrangement, the electrons from the PMN-PT were not able to transfer to the outside so that the electric field can be preserved inside the adsorbents. The details of the experimental setup and blank sorption measurement from the glass container and PMN-PT were described in previous published paper of our group [16].

3. Results and discussion

3.1. Characterization

Fig. 2 shows the XRD spectra of as-synthesized IRMOF8 and the activated carbon composites. The patterns for both pure IRMOF8 and MOFAC composites match with previous data on IRMOF8 reported by Yaghi [28], which proves that the deposition process did not alter the IRMOF8 crystal structure. Compared to the pattern from Yaghi's patent, the differences in relative peak intensities in the powder XRD pattern reveal IRMOF8 samples studies herein contained a partially collapsed framework. The amount of the
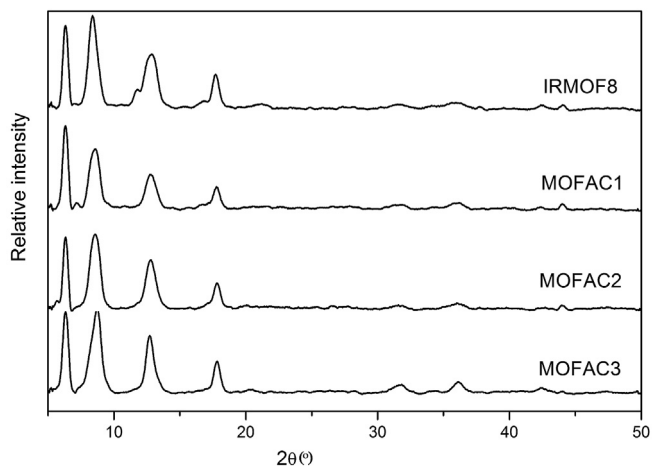
Fig. 2. XRD spectra of pure IRMOF8 and MOFAC composites.

produced structural defects in the lattice increases. The specific surface areas of the samples are characterized by BET. As shown in Table 2, this result consistently supports the measured BET values of the synthesized IRMOF8 and MOFAC composites less than that of Yaghi's sample (1466 m^2 g^{-1}) by the nitrogen sorption because of the different degrees of blockage of the lattice defects acting as a diffusion hindrance to nitrogen molecules.

The TGA analysis (Fig. 3) shows that pure IRMOF8 and the MOFAC composites all exhibit similar weight loss curves upon heating. They started to lose weight due to the removal of moisture and solvent at temperatures above 100 °C. A major weight loss occurred at 400 °C, where thermal decomposition took place. Pure IRMOF8 had a total weight loss of 52.83 wt% at 600 °C. Since activated carbon has nearly zero weight loss upon heating in nitrogen atmosphere, the weight loss of pure MOF was used to calculate the MOF content in the MOFAC composites. As shown in the embedded table in Fig. 3, the MOF wt% in MOFAC1, MOFAC2, and MOFAC3 are 85.32%, 82.23%, and 77.80%, respectively.

Table 1 shows the resistivity, capacitance and dielectric constant of the IRMOF8 and MOFAC composites. As the concentration of carbon increased, the capacitance increased. The insulator to conductor transition was observed at carbon weight fractions between 17.77 wt% to 22.2 wt%. The dielectric constant of the composites as a function of frequency and carbon content is shown in

Table 1
Electrical performance of IRMOF8 and MOFAC composites.

Sample	Carbon content	Resistivity	Capacitance	Dielectric constant
IRMOF8	0	>100 MΩ	0.018 nF	2
MOFAC1	14.68 wt%	>100 MΩ	0.028 nF	4.2
MOFAC2	17.77 wt%	>100 MΩ	0.031 nF	6.5
MOFAC3	22.2 wt%	5.6 MΩ	–	–

Fig. 4. Virgin IRMOF8 has a dielectric constant of 2. The dielectric constant of the composites rises with the increasing carbon fraction. The dielectric constants for both pure MOF and MOFAC composites are frequency independent at room temperature. The composites clearly show the tunable dielectric response from the addition of the activated carbon. The enhancement of the dielectric constant was attributed to the formation of minicapacitor networks [20,24], where the carbon particles were covered by MOF materials forming localized capacitors. The frequency independent dielectric constant confirms the fact the minicapacitor is the only phenomenon [20] for these composites since the space charge polarization is frequency dependent [23]. However, in order to implant charge enhancement of hydrogen storage in MOF materials, a conductive network formed inside the composites is preferred, where space charge polarization [29] on the conductive path could effectively distribute the electrical charges. Therefore, the composites that have passed the insulator–conductor transition would be ideal for charge induced enhancement of hydrogen storage, which was verified from the storage analysis.

The morphology of activated carbon, IRMOF8 and MOFAC composites was investigated by means of SEM; the images are shown in Fig. 5. The surface morphology of the activated carbon (Fig. 5(e)) is relatively smooth and is completely coated with IRMOF8 (Fig. 5(a) and (b)). Direct deposition of MOF materials onto carbon showed uniform particle distribution and good contact, as shown from the SEM analysis (Fig. 5(a) and (b)). The carbon substrates were covered by small spheroids of MOF, which heterogeneously nucleated on the carboxylate groups of the carbon surface, thus forming a strong inter-particle bond and good uniformity. The deposition mechanism is following the theory of heterogeneous nucleation. Homogeneous nucleation of IRMOF8 is likely to proceed via the formation of the so-called secondary building units (SBUs), which in the case of IRMOF8 is a tetrahedral [Zn4O]$^{6+}$ cluster ion with the six Zn···Zn edges bridged by naphthalene linker. These

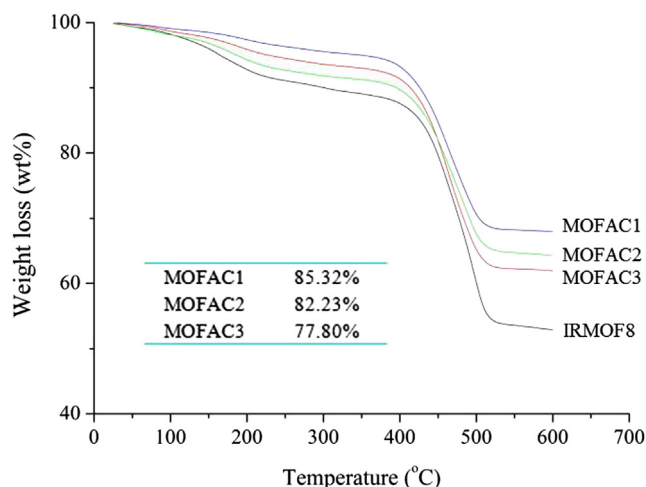|	
MOFAC1	85.32%
MOFAC2	82.23%
MOFAC3	77.80%

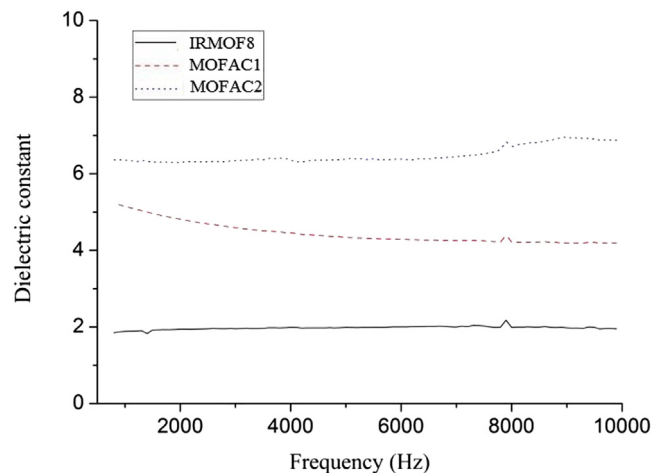**Fig. 3.** TGA curves of pure IRMOF8 and MOFAC composites.

Fig. 4. Dielectric constant of the MOFAC composites at room temperature as a function of frequency.
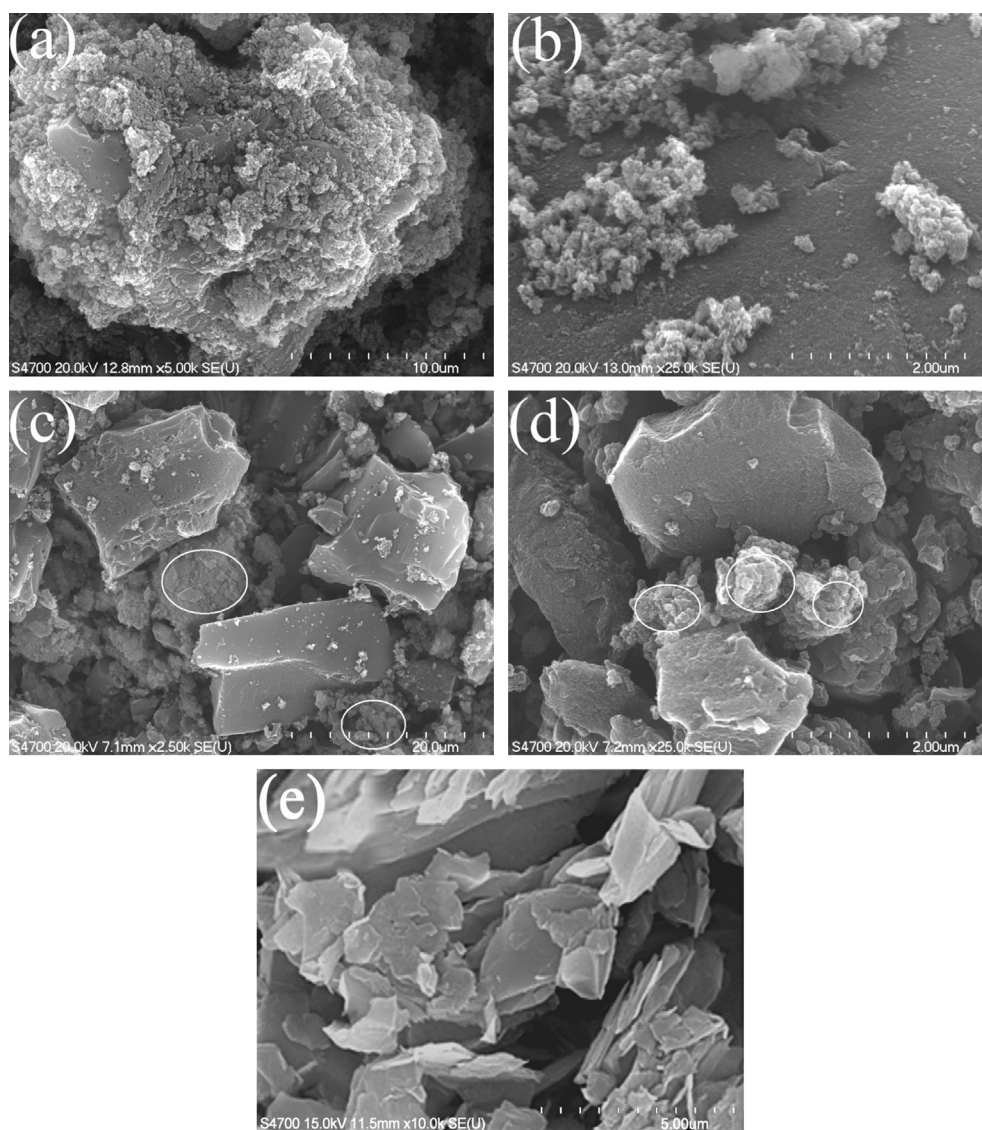
Fig. 5. FE-SEM images of IRMOF8, MOFAC composites and activated carbon. (a) and (b): direct deposition; (c) and (d): mechanical mixing; (e): pure activated carbon.

octahedral connectors then fuse together and form the network and eventually cubic macrocrystals. Directed heterogeneous nucleation on solid substrates should thus be possible if solvated or polynuclear Zn^{2+} complexes, such as SBUs, or even larger IRMOF8 nuclei selectively bind to carbon via a naphthalene linker bridge connected to a surface-bound Zn^{2+} cation [30]. Such mechanism has also been employed in synthesis of MOF/CNT [31] and MOF thin films [30]. Mechanically mixed MOF-carbon composites composed of the same weight ratio of MOFAC composites were also studied to compare the particle distributions. The mechanical MOF-carbon mixture was prepared by ball milling IRMOF8 and activated carbon at a ratio of 4:1 by weight for 30 min. Clear particle separation

Table 2
BET surface areas of IRMOF8, carbon, and MOFAC composites.

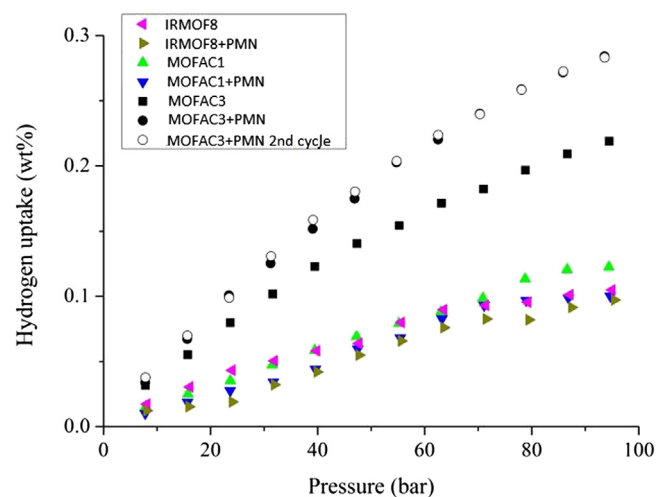| Sample	BET surface area (m^2 g^{-1})	Micropore area (m^2 g^{-1})
IRMOF8	877.24	496.72
Carbon	1791.06	554.49
MOFAC1	898.38	420.47
MOFAC2	943.32	461.80
MOFAC3	990.90	480.83
Yaghi's sample	1466	–

Fig. 6. Hydrogen storage analysis of IRMOF8 and MOFAC composites at 298 K with and without PMN-PT.
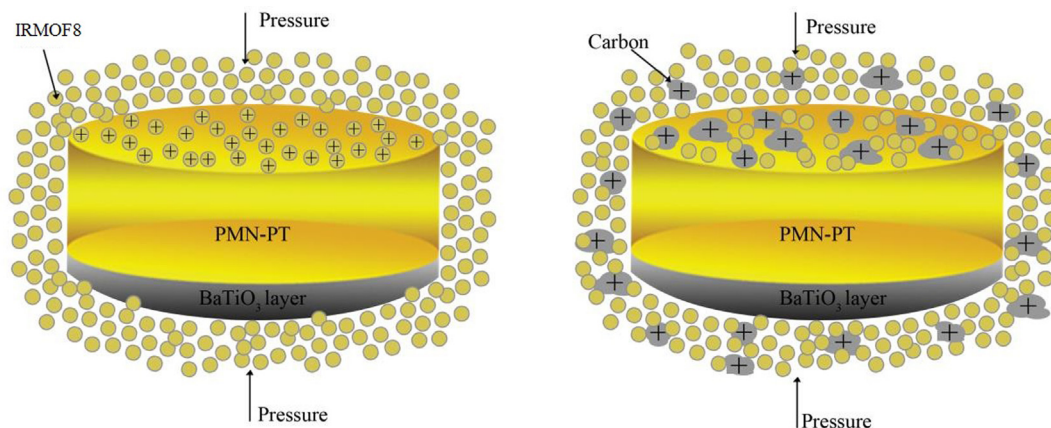
Fig. 7. Schematic of charge distributions in pure IRMOF8 (left) and MOFAC composites (right).

was observed, where the MOF agglomerated together forming large chunks, as highlighted by the white circles in Fig. 5(c) and (d). The MOF particle distribution and MOF-carbon interconnection were poor. Therefore, the direct deposition method showed great advantages not only in the percolative effect, but also in the particle contacts and thus the charge distribution, where ideally every MOF particle could get charge from the nearby carbon particles.

The important issue for synthesizing composites as adsorbents is that the total porosity should not be significantly affected. The total porosity of activated carbon, pure IRMOF8, and MOFAC composites, measured by nitrogen adsorption is listed in Table 2. The large surface area discrepancy between IRMOF8 and carbon ensures that the porosity of the composites increases with increasing carbon content. The uniform deposition ensured the pores to be unblocked and open for gas adsorption.

3.2. Hydrogen adsorption

The hydrogen adsorption isotherm at 298 K is shown in Fig. 6. The weight percentage of hydrogen adsorption shown here was obtained from the net amount of uptake after removal of the uptake on the blank container measurement. Pure IRMOF8 and MOFAC1 both have similar adsorption features and reach 0.1 wt% at 100 bar. With the presence of the charge generator PMN-PT, the enhancement of adsorption was nearly negligible. When the carbon content increased, as in MOFAC3, the storage increased to 0.197 wt% (80 bar), which was due to the contribution from the extra activated carbon. With help from the PMN-PT, the hydrogen uptake was further increased to 0.259 wt% (80 bar), which is about 31.5% enhancement over the MOFAC3. Our previous results [16] presented that hydrogen uptake on pure activated carbon were 0.54 wt% and 0.43 wt% in the presence and absence of the PMN-PT at hydrogen pressure of 80 bar, corresponding to a 30% increase. Based on the weight content of carbon in MOFAC3, the other significant amount of increase was due to the charged MOF materials, which accounted for 31.9% enhancement for MOF. Moreover, the electric field enhancement was fully reversible, as indicated from the second adsorption isotherm of the MOFAC3 sample.

The detailed mechanism is elucidated in Fig. 7. PMN-PT produced a voltage across the positive and negative sides and formed an electric field in response to an applied force. When the PMN-PT was surrounded by IRMOF8, the charges generated from the PMN-PT could not be distributed throughout the whole surface of the sample, but only concentrated on the surface of the positive side. Therefore, the charge induced enhancement of hydrogen adsorption for pure IRMOF8 was negligible. When carbon was induced and worked as a charge distributor, the electrical charges could be

passed along by the contacted activated carbon particles. The IRMOF8 particles could also receive the charges from the adjacent carbon particles. The charge induced electric field implanted on both carbon and IRMOF8 particles, thus forming a localized charge polarization. The induced strong electrostatic force could in turn polarize the incoming hydrogen molecules to form a strong bonding with the hydrogen and enhance the storage uptake. When the composite was not conductive, the charges were not distributed throughout the surface of the sample. Hence, only the conductive composite-MOFAC3 possessed significant charge induced enhancement of hydrogen storage. The optimum condition was not found in this study and future investigations are needed regarding increasing the carbon content further to study the charge effects.

The electrostatic interaction between adsorbent and hydrogen molecules could be enhanced under electric field so that total hydrogen storage could be remarkably increased. It has been the foundation to develop the concept on using electric charges to enhance hydrogen adsorption in a hydrogen system. By simply and safely embedding an electric field generating material PMN-PT into a modified IRMOF8, the experimental work to verify this concept was reported here. In the previous research, spillover is considered as the most effective method to improve hydrogen storage on MOFs dramatically but the application was limited by the slow uptake/release kinetics and desorption and reversibility problems [10]. Compared to the spillover method, the encouraging advantages of electric field enhancement is complete hydrogen desorption during the release process and rapid uptake/release kinetics. The findings from this effort would open a new avenue for development of a high-capacity hydrogen storage system with ideal desorption performance by introducing a safe and simple PMN-PT disc.

4. Conclusion

IRMOF8 has been successfully deposited on activated carbon through heterogeneous nucleation. The dielectric constant of the composites increased with increased carbon content. The charges generated by the PMN-PT were distributed through the composites and the most significant hydrogen storage capacity was 0.259%, which showed a 31.9% increase over the MOFAC3 at 80 bar. This is attributed to an electrostatic interaction between hydrogen and MOFAC3, which was created and helped the storage uptake under an electric field.

References

[1] H. Jin, Y.S. Lee, I. Hong, Catal. Today 120 (2007) 399–406.
[2] M. Bastos-Neto, C. Patzschke, M. Lange, J. Möllmer, A. Möller, S. Fichtner, et al., Energy Environ. Sci. 5 (2012) 8294–8303.
[3] H. Wang, Q. Gao, J. Hu, J. Am. Chem. Soc. 131 (2009) 7016–7022.
[4] G.G. Tibbetts, G.P. Meisner, C.H. Olk, Carbon 39 (2001) 2291–2301.
[5] H. Takagi, H. Hatori, Y. Soneda, N. Yoshizawa, Y. Yamada, Mater. Sci. Eng. B 108 (2004) 143–147.
[6] B. Panella, M. Hirscher, S. Roth, Carbon 43 (2005) 2209–2214.
[7] L. Regli, A. Zecchina, J.G. Vitillo, D. Cocina, G. Spoto, C. Lamberti, et al., Phys. Chem. Chem. Phys. 7 (2005) 3197–3203.
[8] Y.H. Hu, L. Zhang, Adv. Mater. 22 (2010) 117–130.
[9] H. Furukawa, M.A. Miller, O.M. Yaghi, J. Mater. Chem. 17 (2007) 3197–3204.
[10] M.P. Suh, H.J. Park, T.K. Prasad, D.W. Lim, Chem. Rev. 112 (2012) 782–835.
[11] M. Dinca, J.R. Long, Angew. Chem. Int. Ed. 47 (2008) 6766–6779.
[12] Y.W. Li, R.T. Yang, J. Am. Chem. Soc. 128 (2006) 8136–8137.
[13] Y.W. Li, R.T. Yang, J. Am. Chem. Soc. 128 (2006) 726–727.
[14] S. Shi, J.Y. Hwang, X. Li, X. Sun, B.I. Lee, Int. J. Hydrogen Energy 35 (2010) 629–631.
[15] X. Li, J.Y. Hwang, S. Shi, X. Sun, Z. Zhang, Carbon 48 (2010) 876–880.
[16] S. Shi, J.Y. Hwang, X. Li, X. Sun, Energy Fuels 23 (2009) 6085–6088.
[17] Z. Zhang, J.Y. Hwang, C. Wen, X. Li, Int. J. Hydrogen Energy 37 (2012) 16018–16024.
[18] W. Liu, Y.H. Zhao, J. Nguyen, Y. Li, Q. Jiang, E.J. Lavernia, Carbon 47 (2009) 3452–3460.
[19] L. Wang, Z.M. Dang, Appl. Phys. Lett. 87 (2005) 042903.
[20] Q. Chen, P.Y. Du, L. Jin, W.J. Weng, G.R. Han, Appl. Phys. Lett. 91 (2007) 022912.
[21] Z.M. Dang, J.P. Wu, H.P. Xu, S.H. Yao, M.J. Jiang, J. Bai, Appl. Phys. Lett. 91 (2007) 072912.
[22] K. Ahmad, W. Pan, S.L. Shi, Appl. Phys. Lett. 89 (2006) 133122.
[23] S.L. Shi, J. Liang, J. Am. Ceram. Soc. 89 (2006) 3533–3535.
[24] S.H. Yao, Z.M. Dang, M.J. Jiang, J.B. Bai, Appl. Phys. Lett. 93 (2008) 182905.
[25] L.M. Huang, H.T. Wang, J.X. Chen, Z.B. Wang, J.Y. Sun, D.Y. Zhao, et al., Microporous Mesoporous Mater. 58 (2003) 105–114.
[26] B. Panella, M. Hirscher, Adv. Mater. 17 (2005) 538–541.
[27] Z. Zhang, J.Y. Hwang, C. Wen, X. Li, J. Power Sources 236 (2013) 158–162.
[28] O.M. Yaghi, M. Eddaoudi, H. Li, J. Kim, N. Rosi, U.S. Patent no. 6,930,193 B2, 2005.
[29] J.Q. Huang, P.Y. Du, W.J. Weng, G.R. Han, J. Inorg. Mater. 20 (2005) 1106–1112.
[30] S. Hermes, F. Schroder, R. Chelmowski, C. Woll, R.A. Fischer, J. Am. Chem. Soc. 127 (2005) 13744–13745.
[31] S.J. Yang, J.Y. Choi, H.K. Chae, J.H. Cho, K.S. Nahm, C.R. Park, Chem. Mater. 21 (2009) 1893–1897.